Desalination and Water Treatment
www.deswater.com

doi: 10.5004/dwt.2023.29207

283 (2023) 62–73
January

Preparation of an enhanced chitosan modified flocculant with both chelation adsorption and flocculation effects for efficient treatment of Pb^{2+} heavy metal wastewater

Lixiu Liu*, Aijiang He

College of New Energy and Battery, Yibin Vocational Technical College, Yibin 644003, China, emails: liulixiu2020@163.com (L. Liu), aijianghe@163.com (A. He)

Received 23 August 2022; Accepted 9 December 2022

ABSTRACT

In this study, chitosan (CS), acrylamide (AM) and itaconic acid (IA) were selected as raw monomers to prepare a novel flocculant CS-g-P(AM-IA) for heavy metals' removal. CS-g-P(AM-IA) are rich with carboxylic acid ionic groups through ultrasonic-free radical initiated polymerization. The CS-g-P(AM-IA) has both chelation coordination and flocculation effect, which is used for removing heavy metal Pb^{2+} efficiently. The effects of one-factor experimental preparation conditions such as initiator concentration, total monomer concentration, total mono-chitosan mass ratio and ultrasound time on the intrinsic viscosity of CS-g-P(AM-IA) were investigated. Thus, the optimization of ultrasonically initiated CS graft polymerization mechanisms and preparation conditions will be further understood and explored. The results of Fourier-transform infrared spectroscopy, thermogravimetry/differential scanning calorimetry (TG/DSC) and scanning electron microscopy (SEM) indicated that CS was successfully grafted by AM and IA. In addition, TG/DSC and SEM analyses showed that CS-g-P(AM-IA) had better thermal stability and rougher surface topography, respectively. The chelating–flocculation experimental results showed that the removal rate of Pb^{2+} reached 84.5% and 64.3% by CS-g-P(AM-IA) and CS at pH = 5.0, flocculation time of 25 min, flocculant dosage of 3.0 mg/L, respectively. The Pb^{2+} removal effect by CS-g-P(AM-IA) was obviously superior than that of CS. The ionic strength and coexisting positive ions have an adverse effect on the adsorption performance for the flocculants, and the effect of Ca^{2+} was obvious. Pb^{2+} ions were mainly immobilized by CS-g-P(AM-IA) through chelation and flocculation by its IA carboxyl groups. And then it was generated large and dense heavy metal flocs (d_{50} = 275.9 μm, D_f = 1.91) by adsorption bridge, net trapping and sweeping to enhance the separation and removal performance of Pb^{2+} ions.

Keywords: Chitosan; Itaconic acid; Heavy metal wastewater; Flocculant; Graft polymerization

1. Introduction

With the accelerating industrialization and urbanization, water pollution has become a serious environmental problem, which has attracted global attention. Industrial production produces a large amount of heavy metal wastewater, which is discharged into the water ecosystem and poses a great threat to the environment and human life. Heavy metal ions are difficult to biodegrade, and can accumulate in living organisms. And then, it accumulates in the human body through the food chain, as well as exists in certain organs for a long time, causing chronic poisoning [1,2]. The electroplating industry, battery manufacturing, the mining industry, the metal refining industry and

* Corresponding author.

the forging industry produce a considerable amount of high concentrations of lead ions (Pb^{2+}) wastewater in the production and application processes, which may cause lung disease, kidney disease, hepatitis, encephalopathy or central nervous system disorders, etc. [3]. For the sake of ecological safety and human health, an advanced water treatment technology is urgently needed to efficiently treat heavy metal (Pb^{2+}) wastewater.

The methods to remove the heavy metal wastewater containing Pb^{2+} mainly include chemical precipitation, membrane filtration, ion-exchange, adsorption, etc. [4–7]. Among them, flocculation is a commonly used method that has received a lot of attention because of its facile operation and application, high efficiency, low costs and energy requirements [8,9]. The ability of coagulant or flocculant to remove pollutants depends on its molecular weight, the type and number of functional groups and also the number of charges that it presents [10]. Chitosan (CS) is the only amino weak base polysaccharide in nature, and its molecular chain contains a large number of amino groups ($–NH_2$) and hydroxyl groups (–OH), allowing it to chelate well with heavy metals [11]. Furthermore, these active sites of amino ($–NH_2$) and hydroxyl (–OH) groups can facilitate the grafting of different functional groups by means of hydrogen or ionic bonds. Thus, it provides an important way to prepare functionally enhanced polymer modified chitosan-based heavy metal flocculants [12]. Therefore, CS is widely used in various water treatment fields. In addition, carboxylate anionic groups have strong affinity and coordination to heavy metal ions. Additional, itaconic acid (IA) is a dicarboxylic acid vinyl organic monomer that can be obtained from algal fermentation and is widely used in the modification of natural products such as starch, alginate, cellulose, and CS [13]. IA contains ethylene bonds that facilitate initiation of polymerization, and it is easy to copolymerize with other monomers and form polymers rich in carboxyl groups, and the prepared polymer has strong chelating and adsorption ability [14,15]. IA can be grafted onto the side chain of CS by polymerization and modification to prepare a heavy metal flocculant with both chelating and flocculation effect, which can be used for efficient treatment of Pb^{2+} heavy metal wastewater. Ultrasound vibrating at frequencies between 20 KHz and 10 MHz can produce cavitation when it penetrates the medium [16,17]. Ultrasonic chemical reaction is a technique that uses the ultrasonic cavitation effect to accelerate and control chemical reactions, thereby moderating the reaction conditions and shortening the reaction time [18]. In addition, ultrasonic has mechanical effects such as oscillation, emulsification, diffusion, etc. It can play a role in accelerating the heat and mass transfer process of the reaction system as well as promoting chemical reactions [19,20]. Therefore, the application of ultrasonic-initiated polymerization technology is a better choice to be applied in the grafting and polymerization of CS based polymers and flocculants.

Therefore, in this study, a new heavy metal flocculant CS-g-P(AM-IA) is to prepared by ultrasonic-initiated copolymerization of IA, acrylamide (AM) and CS. CS-g-P(AM-IA) was used to treat Pb^{2+} heavy metal wastewater efficiently. The effect of single-factor preparation conditions on CS-g-P(AM-IA) synthesis was investigated. The effect of IA carboxyl groups on the adsorption flocculation process was also examined by comparing the removal effects of various flocculants. The effects of flocculant dosage, pH, flocculation time, ionic strength and coexisting cations on the removal of Pb^{2+} were investigated to evaluate their chelating flocculation performance. Furthermore, the floc structure (particle size and fractal dimension) characteristics of the generated heavy metal chelated flocs was studied to further discuss the related chelating flocculation mechanism.

2. Experiment

2.1. Experimental materials and instruments

AM, CS and IA were all purchased from Sinopharm Chemical Reagent Co., Ltd., (Shanghai, China). Anhydrous ethanol and acetone were provided by Chongqing Chuandong Chemical Industry Co., Ltd., (Chognqing, China). The initiator V50 was purchased from Shanghai Ruilong Biochemical Co., Ltd., (Shanghai, China). The anhydrous ethanol and acetone were gifts from Sichuan Yuansongda Chemical Co., Ltd., (Zigong, China). The pH of the reaction solution was adjusted using HCl solution and NaOH solution at a concentration of 0.1 mol/L, and measured with a pH meter (S40, Mettler-Toledo, Switzerland). The ubbelohde viscometer is purchased from Shanghai Jinghong Experimental Equipment Co., Ltd., (Shanghai, China). The N_2 (purity ≥99.999%) used for the experiments was provided by Sichuan Runtai Special Gas Supply Company (Chengdu, China).

2.2. Polymer preparation

The flocculant CS-g-P(AM-IA) was synthesized by grafting copolymerization in an ultrasonic initiator using CS, IA and AM as raw materials and V50 as an initiator. The reaction path is shown in Fig. 1. First, a certain amount of CS was weighed and dissolved in a dilute acetic acid solution (mass fraction: 1.0 wt.%) to prepare an aqueous CS solution (mass fraction: 3.0–7.0 wt.%). Then a certain mass of AM and IA (m_{AM}:m_{IA} = 4:1) and a predetermined volume of aqueous CS solution were added to the 200 mL reaction flask according to the composition ratio requirement, and shaken well to a homogeneous solution. The pH of the reaction solution was adjusted to 5.0, and the reaction flask was charged with N_2 for 20 min, and then a set amount of initiator V50 aqueous solution was added. The reaction flask was then quickly sealed and placed in an ultrasonic device (power: 500 W, frequency: 40 KHz, adjustable range: 40%~100%) for reaction. In this study, the ultrasonic power was 300 W. After a period of ultrasonic radiation (9 min), the reactor was closed and the reaction flask was removed and aged for 2 h. The product was then purified with anhydrous ethanol and acetone. The purified product was then dried in a constant temperature oven set at 90°C until the mass no longer changed and ground for usage.

2.3. Polymer characterization methods

For Fourier-transform infrared spectroscopy (FT-IR) analysis, the experiments were performed by KBr press method, and the infrared absorption spectra of the samples

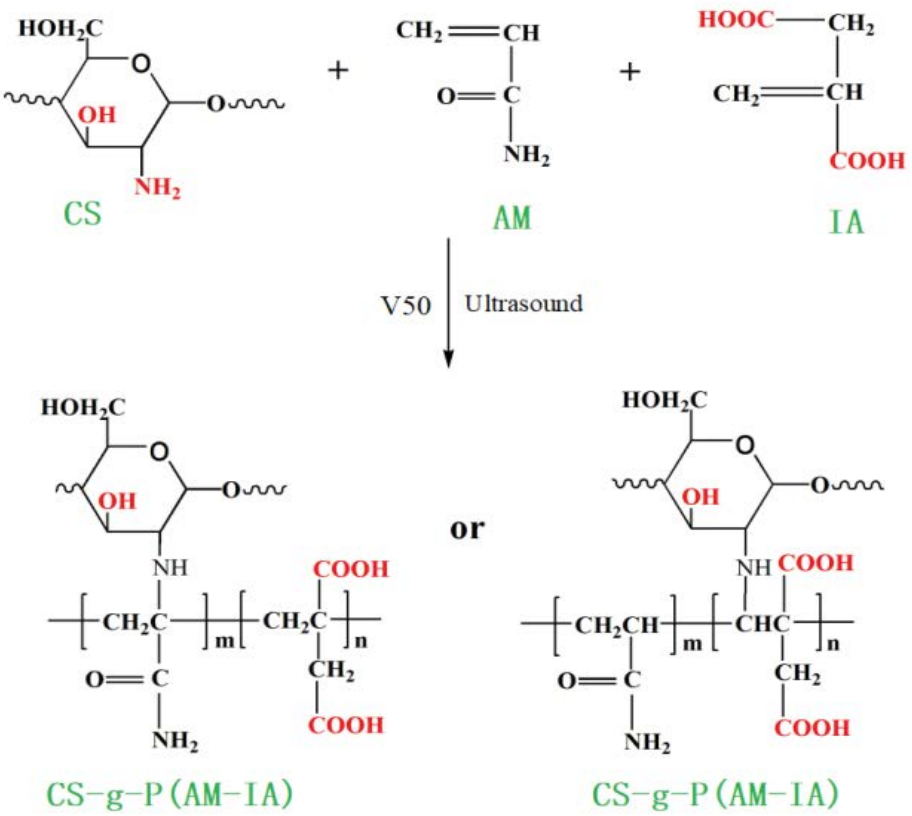

Fig. 1. Synthesis route of CS-g-P(AM-IA).

at 400~4,000 cm^{-1} were recorded by Series II 550 of Mettler-Toledo Instruments Ltd. in Switzerland. After samples were gold sprayed with an Emitech sputtering ion coater, their surface morphologies were observed with a scanning electron microscope of the MIRA 3 LMU type from TESCAN, Czech Republic. For thermogravimetry/differential scanning calorimetry (TG/DSC) analysis, the samples were analyzed for weight loss in a temperature range of 30°C–600°C on a DTG-60H thermal analyzer from Shimadzu Instruments, Japan, under the operating conditions of nitrogen atmosphere and a temperature rise rate of 10°C/min. The polymer intrinsic viscosity ([η]) is commonly measured using the capillary viscometer method [21,22].

2.4. Flocculation experiment

The concentration of Pb^{2+} in the Pb^{2+} heavy metal wastewater was 50.6 mg/L, COD was 32.9 mg/L, and turbidity was 11.3 NTU. The flocculants were configured into a solution with a concentration of 0.2 g/L and diluted according to the experimental requirements. And then, it was used for subsequent batch experiments to investigate the adsorption and coagulation effects on the Pb^{2+} heavy metal wastewater. The pH of the system was adjusted with aqueous solutions of hydrochloric acid and sodium hydroxide at a concentration of 0.1 mol/L. The effect of pH on the Pb^{2+} ions removal was investigated in the range of 2.0~10.0, respectively. The concentration of Na^{+} ions was set from 0 to 100 mmol/L, and the concentrations of coexisting cations K^{+}, Ca^{2+} and Mg^{2+} were all 50 mol/L. The effects of ionic strength and coexisting cations on the adsorption and flocculation effect were examined. TS6-1 program-controlled experimental stirrer was used to stir 1 L of Pb^{2+} wastewater at 300 rpm for 2 min, followed by slow stirring at 60 rpm for 5–30 min. Then, a certain amount of water sample was extracted with a 0.22 μm syringe filter to examine the Pb^{2+} concentration. The concentration of Pb^{2+} in the solution was determined by dithizone photometric method. The removal efficiency of Pb^{2+} by flocculants was expressed as E(%) and calculated as follows.

$$E(\%) = \frac{C_0 - C_e}{C_0} \times 100\% \quad (1)$$

where E(%) is adsorption removal efficiency, and C_0 is the initial concentration of Pb^{2+}, C_e is the concentration of Pb^{2+} after flocculation.

3. Results and discussion

3.1. Polymerization

3.1.1. Influence of V50 concentration

The initiator V50 used in the experiment is a water-soluble azo initiator, which has the advantages of stable initiation property and good water solubility. At the same time, the V50 decomposition follows a first-order reaction and the free radicals from V50 have high initiation efficiency

[23]. The V50 molecular structure possesses N–N double bond, and it is relatively weak and easy to break and form free radicals during the reaction process to initiate polymerization. Therefore, the V50 concentration will affect the graft copolymerization. When the polymerization condition remains at total monomer concentration of 30 wt.%, the $m_{(AM+IA)}/m_{CS}$ of 4, and the ultrasound time of 9 min, the V50 concentration influence on the product intrinsic viscosity was investigated. In Fig. 2a, it can be found that the intrinsic viscosity showed an increasing trend with the gradual increase of V50 concentration. At V50 concentration of 6 mol/L, the intrinsic viscosity for CS-g-P(AM-IA) reached the maximum value of [η] = 5.54 dL/g. When it exceeds 6 mol/L, the intrinsic viscosity of CS-g-P(AM-IA) slowed a down trend until 9 mol/L. Appropriate high initiator concentration is beneficial to the smooth progress of polymerization and grafting reaction. The role of V50 in the polymerization reaction is to decompose and form free radicals, so that CS can generate active sites, and then AM and IA can be grafted with these active groups [24,25]. In the initial polymerization stage, the number of free radicals generated by V50 are relatively lack, and which is not conductive to attack CS and produce sufficient active sites for graft polymerization. The less active sites on CS molecular chain make AM and IA unable to polymerize with CS efficiently. As a result, the polymerization rate is low, and the CS-g-P(AM-IA) intrinsic viscosity is relatively low. When the V50 concentration increased further, the free radical production increased as well, which is favorable for the chain growth process. The CS-g-P(AM-IA) intrinsic viscosity is also increased, and its long-chain polymer formed. When the V50 concentration is too high, the initiator breaks down rapidly to form a large number of free radicals in a short period of time. On the one hand, a large number of free radicals will cause a fierce copolymerization and crosslinking reactions between the monomers. It quickly causes the termination of chain growth and grafting, and also reduce the intrinsic viscosity of the product. On the

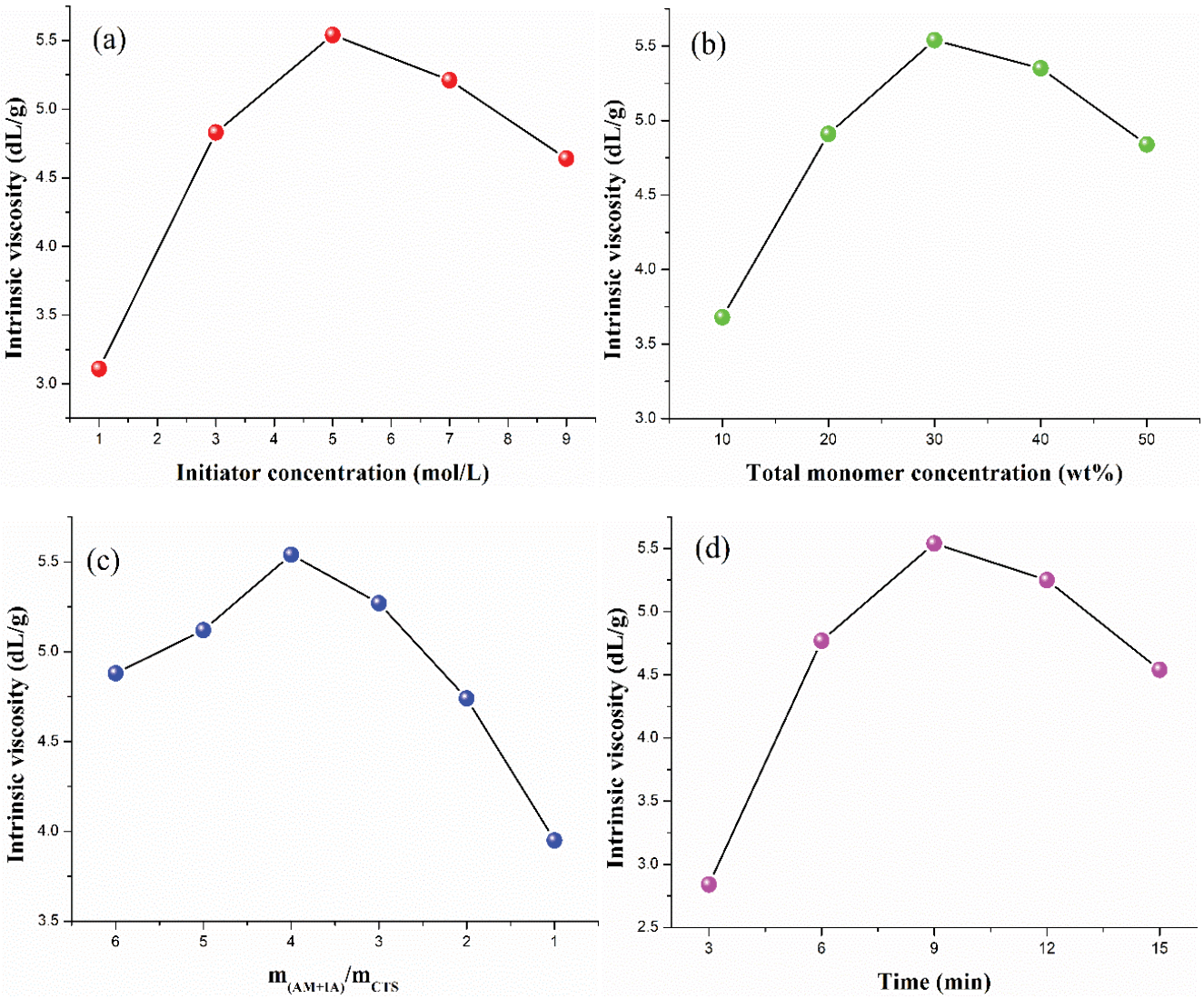

Fig. 2. Effects of V50 concentration (a), total monomer concentration (b), $m_{(AM+IA)}/m_{CS}$ (c) and ultrasonic time (d) on the intrinsic viscosity of CS-g-P(AM-IA).

other hand, the coupling reaction will occur between the excess free radicals. It results in the chain termination rate being far greater than the chain growth rate, thus terminating the polymerization reaction. At the same time, a large number of free radicals make the number of active sites generated by the activation of CS far exceed the number of AM and IA monomers. CS itself will also undergo self-polymerization, reducing the intrinsic viscosity of the final product [26,27]. Therefore, 6 mol/L of V50 is more suitable for CS-g-P(AM-IA) preparation.

3.1.2. Influence of total monomer concentration

The total monomer concentration determines the number of grafted and polymerized monomers. Therefore, the effect of the total monomer concentration on the CS-g-P(AM-IA) intrinsic viscosity was investigated. The other conditions of the polymerization reaction were maintained as the V50 concentration of 6 mol/L, $m_{(AM+IA)}/m_{CS}$ of 4 and the ultrasonic time of 9 min. It can be seen from Fig. 2b that during the increase of total monomer concentration, the CS-g-P(AM-IA) intrinsic viscosity increases first and then reduces. When the total monomer concentration is 30 wt.%, the removal rate reaches the maximum value ([η] = 5.54 dL/g). The total monomer concentration will directly affect the number of free AM and IA radicals generated at the beginning of the reaction. When the total monomer concentration is low, the amounts of free AM and IA radicals generated is relatively not rich [28]. In addition, the collision probability between monomers and free V50 radicals is relatively low. Consequently, the grafting and the chain growth process doesn't proceed well to obtain the high intrinsic viscosity of the synthesized product. As the total monomer concentration increased, the number of free AM and IA radicals and the collision probability of monomers grew. On this condition, the chain growth process and the reaction rate of graft polymerization are accelerated, which was conducive to increasing the intrinsic viscosity and graft rate of the product [29]. However, when the total monomer concentration increases to a certain value (30 wt.%), the explosion reaction will happen among monomers or between monomers and V50 free radicals. This will cause the temperature of the reaction system to rise sharply, resulting in chain transfer or chain termination. At the same time, the crosslinking between monomers further reduces the polymer water solubility, which is not conducive to the polymerization reaction [30]. So, the intrinsic viscosity may be reduced to different degrees by high total monomer concentration. The preferred total monomer concentration is select as 30 wt.% in this study.

3.1.3. Influence of $m_{(AM+IA)}/m_{CS}$

As the main grafted matrix, CS has an important impact on the graft rate and the number of monomers that can be loaded, and finally affects the intrinsic viscosity of the product. When the polymerization reaction conditions at initiator concentration of 6 mol/L, the total monomer concentration of 30 wt.%, and the ultrasonic time of 9 min, the influence of $m_{(AM+IA)}/m_{CS}$ on the intrinsic viscosity of the product was investigated. In Fig. 2c, with the decrease of the $m_{(AM+IA)}/m_{CS}$ ratio, that is, the increase of the CS content, the intrinsic viscosity increases of CS-g-P(AM-IA) first and then decreases. When $m_{(AM+IA)}/m_{CS}$ is of 4, the grafted polymer intrinsic viscosity reaches its maximum value ([η] = 5.54 dL/g). The results showed that the relative high amount of CS was beneficial to increase the intrinsic viscosity of the grafted product. The CS graft copolymerization with AM and IA occurs at their contact interface. When CS content is relatively low, the effective active sites that can be copolymerized are limited, and the number of monomers that can be grafted is limited. With the increase of CS content, the number of active sites in the system increases, which can fully contact and collide with monomers to proceed polymerization reaction [31]. It is conducive to chain growth, and thus improving the intrinsic viscosity of the product. In addition, monomers AM and IA contain rich olefin double bonds and are easy to polymerize. It is necessary to appropriately increase the total monomer ratio of AM and IA to facilitate the chain growth reaction and the graft polymerization. However, when $m_{(AM+IA)}/m_{CS}$ exceeds a certain range, the number of grafted CS decreases correspondingly, a large number of ineffective active sites appear on AM and IA, and the grafting rate decreases significantly. At the same time, due to CS poor solubility, too much CS will reduce the solubility of the product, thus reducing the effectiveness of graft copolymerization. In addition, the increase of AM and IA evidently hinders the effective contact between the monomers and the active site in CS, resulting in the decrease of the intrinsic viscosity of the product as well as its yield [32–34]. In conclusion, it is appropriate to select $m_{(AM+IA)}/m_{CS}$ as 4.

3.1.4. Influence of ultrasonic time

The initiation method is ultrasonic initiation, so the ultrasonic time also has an evident impact on the product preparation. The other conditions of the polymerization reaction were controlled at V50 concentration of 6 mol/L, the total monomer concentration of 30 wt.%, and $m_{(AM+IA)}/m_{CS}$ of 4. The effect of ultrasonic time on the intrinsic viscosity of the graft polymerization product was analyzed. It can be seen from Fig. 2d that when the ultrasonic time is changed from 3 min to 9 min, the polymer intrinsic viscosity shows an obvious increasing trend, and it reaches the maximum value of 5.54 dL/g. Subsequently, the intrinsic viscosity reduced when the ultrasonic time was extended 9 min. At the initial stage of ultrasound, a large number of free radicals are generated by ultrasonic cleavage V50, which promotes the collision of free radicals with AM, IA and CS [35]. Thus, it leads to grafting and polymerization. The number of generated free radicals increased gradually, the polymerization continued, and the product viscosity increased accordingly. But with the extension of ultrasonic time from 9 min to 15 min, the amount of V50 used to produce initial free radicals are consumed quickly, the amount of subsequently formed free IA and AM radicals decreased, and the reaction rate slowed down. In addition, when the ultrasonic time is too long, the ultrasonic generates a large amount of heat is not easy to emit, prone to the phenomenon of burst and implosion [35–37]. This will also affect the stable and orderly

progress of the polymerization reaction, hinder the chain growth, and make the chain termination happen earlier. Therefore, the optima ultrasound time is chosen as 9 min.

3.2. Polymer characterization

3.2.1. FT-IR analysis

The FT-IR spectra of the flocculants CS-g-P(AM-IA) and CS were displayed in Fig. 3. The strong absorption peaks in CS located at 1,665; 1,155 and 1,081 cm^{-1} corresponded to the –N–H, glycosidic bond (C–O–C) and primary alcohol (C–OH) bending vibrations, respectively [38]. And these characteristic absorption peaks of CS were also found in CS-g-P(AM-IA). In the FT-IR spectra of CS-g-P(AM-IA), the broad absorption peak at 3,443 cm^{-1} corresponds to the O–H stretching vibration peak, and the strong absorption peak appearing at 2,938 cm^{-1} corresponds to the asymmetric stretching vibration of methyl-CH_2 in mono-substituted amides [39]. The characteristic absorption peaks at 1,575 and 1,391 cm^{-1} are assigned to the C=O stretching vibration of IA carboxyl group and the C–N stretching vibration of AM amide group, respectively [40,41]. From the above analysis results, it is clear that the FT-IR spectra of the chitosan graft-modified polymer CS-g-P(AM-IA) show the characteristic absorption peaks of CS, IA and AM, thus indicating that the polymer CS-g-P(AM-IA) is successfully polymerized from AM, CS and IA.

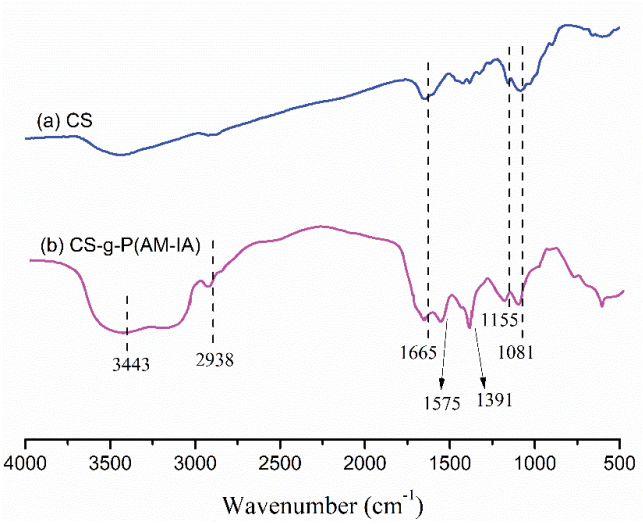

Fig. 3. FT-IR spectrum of the flocculants.

3.2.2. TG/DSC analysis

Fig. 4 displays the thermal gravimetric curves of (a) CS and (b) CS-g-P(AM-IA). As shown in Fig. 4, it can be seen that two stages of weight loss occurred for CS, while three stages of weight loss occurred for CS-g-P(AM-IA). The end point temperature of the first weight loss stage for CS was 85.6°C and the weight loss was 2.8%, while CS-g-P(AM-IA) had an endpoint temperature of 73.4°C for the first stage of weight loss and a weight loss rate of 9.4%. The analysis suggests that the first stage of weight loss is caused by the evaporation of water adsorbed by the hydrophilic groups of the polymer [42]. In the second weight loss phase, CS-g-P(AM-IA) showed three significant heat absorption peaks at temperatures 219.3°C, 276.9°C and 323.8°C, which triggered a weight loss rate of up to 20.3%. However, CS only showed a large heat absorption peak at 279.3°C, which caused an evident weight loss of 54.7%. The analysis suggests that the weight loss in the second-stage may be due to part of the CS molecular backbone decomposition, the amide group imidation reaction, and the pyrolysis thermal decomposition of IA carboxyl group [43]. In addition, the starting temperature of the third weight loss of the polymer CS-g-P(AM-IA) is at 321.5°C, with a weight loss of 37.6%, and its corresponding heat absorption peak occurs at 436.7°C. This part is mainly caused by the decomposition of the C–C bonds of the CS, PAM and IA polymerization molecule backbone in the product [44]. In summary, CS-g-P(AM-IA) presents different thermal properties from CS due to the addition of groups such as AM amide group and IA carboxyl group, which corresponds to its molecular structure and chemical properties. In addition,

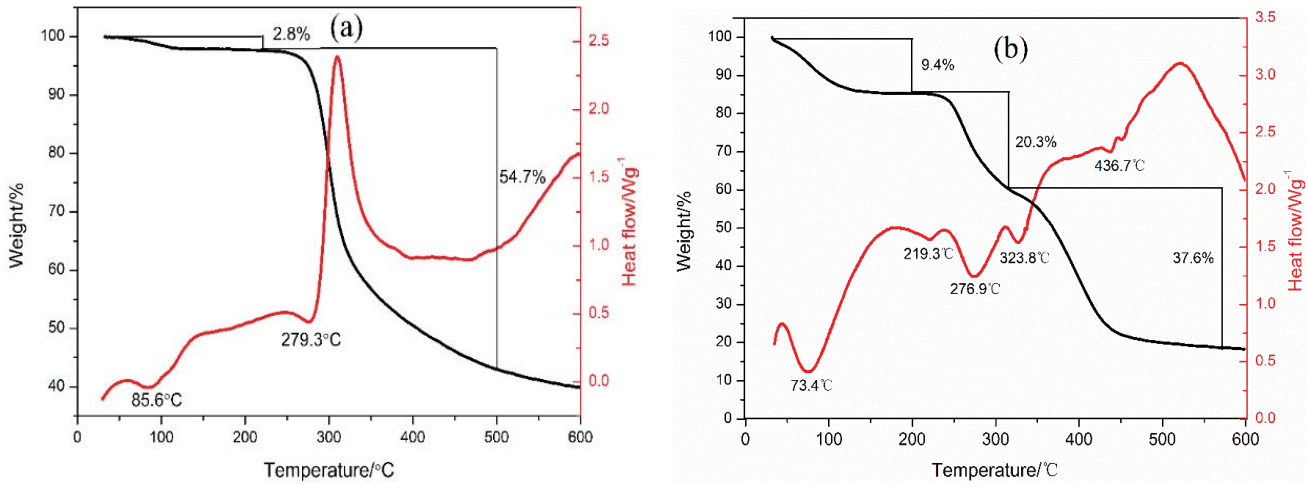

Fig. 4. TG/DSC analysis of CS (a) and CS-g-P(AM-IA) (b).

the onset of thermal decomposition of the polymer is near to 219.3°C, so it can be inferred that CS-g-P(AM-IA) has good thermal stability and hardly decomposes during regular use as well as storage and transport [45].

3.2.3. Scanning electron microscopy analysis

The scanning electron microscopy (SEM) and fractal dimensional analysis results of the graft copolymers CS-g-P(AM-IA) and CS are illustrated in Fig. 5. From the results in this figure, it is clear to see that the surface morphology of these two polymers shows an evident difference. The CS surface morphology has fewer bumps but it is relatively smooth. Meanwhile, there are also no holes were found at its surface. However, the surface of CS-g-P(AM-IA) after graft copolymerization is rough and has more folds, grooves and holes. It is because the fact that the introduced AM and IA monomers collapse the original ordered structure of CS crystals and form folds with varying levels of surface. Thus, it increases the polymer specific surface area and makes its surface rough and uneven. Obviously, it means that CS-g-P(AM-IA) has irregular and distinctly folded and raised surface and will possesses a larger specific surface area. The above-results agree with the direct observation of SEM images. It has been shown that the morphological changes of CS derivatives after grafting are to some extent related to the improvement of their solubility, flocculation and adsorption properties [46,47].

3.3. Chelating and flocculation performances

3.3.1. Effect of dosage

The effect of CS and CS-g-P(AM-IA) dosage on the flocculation and removal performance of Pb^{2+} was investigated at a stirring time of 25 min and pH of 5.0. The results are shown in Fig. 6. With the rising of flocculant dosage, the

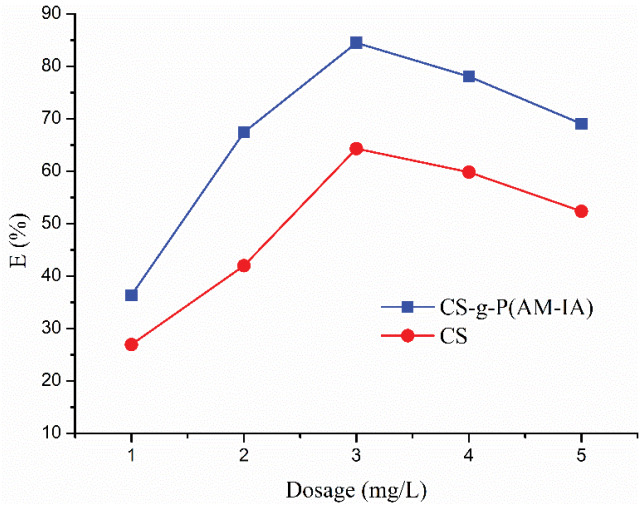

Fig. 6. Effect of flocculant dosage on the Pb^{2+} removal.

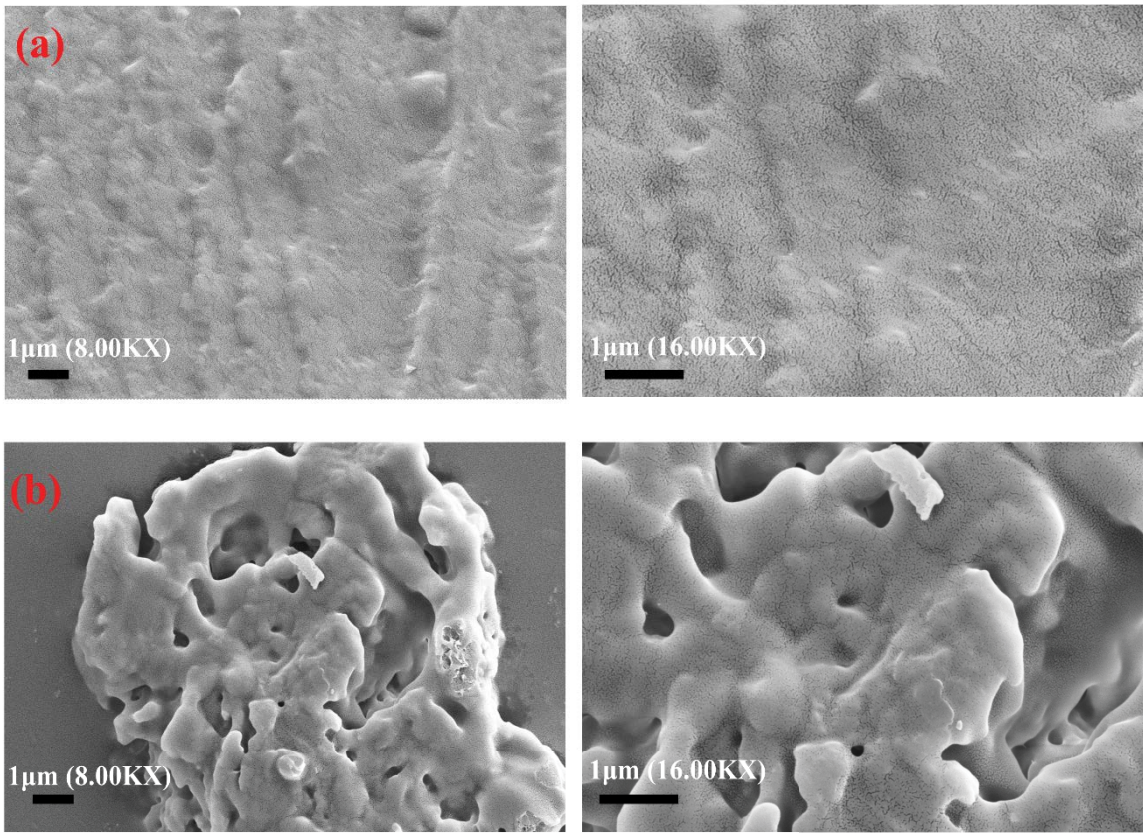

Fig. 5. Morphology analysis of CS (a) and (b) CS-g-P(AM-IA).

removal rate of Pb^{2+} increased rapidly at first and then gradually became smooth. The desirable removal performance (E = 64.3% and 84.5%) were obtained when both CS and CS-g-P(AM-IA) were dosed at 3.0 mg/L. A less dosage resulted in insufficient active sites for Pb^{2+} chelation and flocculation. However, excessively higher dosage resulted in a stronger entanglement of flocculants with each other, which is not conducive to the extension of molecular chains. Last but not least, the generated small flocs of heavy metals were wrapped with an excessive amount of flocculant on their surface, which exposed fewer active sites and were not conducive to improve the adsorption and bridging effect [48]. Both flocculants have effects on the Pb^{2+} removal, while CS-g-P(AM-IA) is significantly more effective than CS. Base on the above analytical results, the optimum flocculant dosage was selected as 3.0 mg/L.

3.3.2. Effect of pH

The stirring time and flocculant dosage was set at 3.0 mg/L and 25 min, respectively. The effect of pH on the removal of Pb^{2+} was investigated and the results are displayed in Fig. 7. The removal efficiency of CS-g-P(AM-IA) for Pb^{2+} exceeded over 75.0% over the pH range of 4.0–8.0, and the relative best removal rate was obtained at pH = 5.0 (E = 84.5%). The optimum pH range for CS was 4.0–7.0 and the relative best Pb^{2+} removal rate was also obtained at pH = 5.0 (E = 64.3%). Under the same pH conditions, the adsorption capacity of CS-g-P(AM-IA) was significantly better than that of CS, which indicated that the carboxyl groups in IA played a key role for the adsorption of Pb^{2+}. The carboxyl groups not only provide abundant points for Pb^{2+} anchoring and cations, but also promote electrostatic interactions and ion-exchange effects with the divalent cation Pb^{2+} by its own strong negative charge. The flocculation capacity of both CS-g-P(AM-IA) and CS exhibited a high pH dependence, and the Pb^{2+} adsorption and removal performance was not satisfactory under strong acid conditions. On the one side, under acidic condition, the zeta potential of the flocculant is positive to cause a stronger mutual repulsion with Pb^{2+} ions, which is not conducive to the electrostatic attraction effect. Meanwhile, H^+ occupied most of the active adsorption sites on the flocculant molecular chain. There are also a certain electrical repulsion between H^+ and Pb^{2+}, which means that less Pb^{2+} ions are adsorbed onto the flocculants [49]. In addition, during the flocculation process, the Pb^{2+} removal efficiency decreases under alkaline conditions. Pb^{2+} forms soluble hydroxyl complexes to consume a large number of active sites, resulting in a decrease in the removal of Pb^{2+} ions [50]. However, under strong alkaline condition, the solubility of CS will become deteriorative, as well as the chemical stability of CS-g-P(AM-IA), which reduced flocculation ligand adsorption and chelate ability. Therefore, the optimum pH value for chelate and flocculation experiments is 5.0.

3.3.3. Effect of flocculation time

The effect of flocculation time on the adsorption and removal of Pb^{2+} ions was investigated at a pH of 5.0 and a flocculant dosage of 3.0 mg/L, and the results were shown in Fig. 8. The removal efficiency of Pb^{2+} by CS-g-P(AM-IA) was so rapid (E = 72.6%) after 15 min, whereas that of CS is very low (E = 35.5%). Then, the Pb^{2+} removal rate continued to increase and reached a maximum value at 25 min, with an optimum removal rate of 84.5% and 64.3% by CS-g-P(AM-IA) and CS, respectively. The initial Pb^{2+} rapid adsorption and removal is mainly due to the strong interactions between the target contaminant and the amino, hydroxyl and carboxyl reactive ionic groups. It makes Pb^{2+} ions to be rapidly captured, adsorbed and immobilised onto CS-g-P(AM-IA) [51]. Compared with CS, the Pb^{2+} adsorption and removal efficiency is more favorable, which can be attributed to the fact that the oxygen-containing functional groups in the polycarboxylic acid provide more surface ligand adsorption sites and stronger electrostatic attraction for the attachment and complexation of Pb^{2+} ions, as well as induce stronger initial adsorption and chelation. Meanwhile, CS-g-P(AM-IA) has longer molecular chains that freely extend in the aqueous phase, and these longer molecular chains provide enough active sites for adsorbing

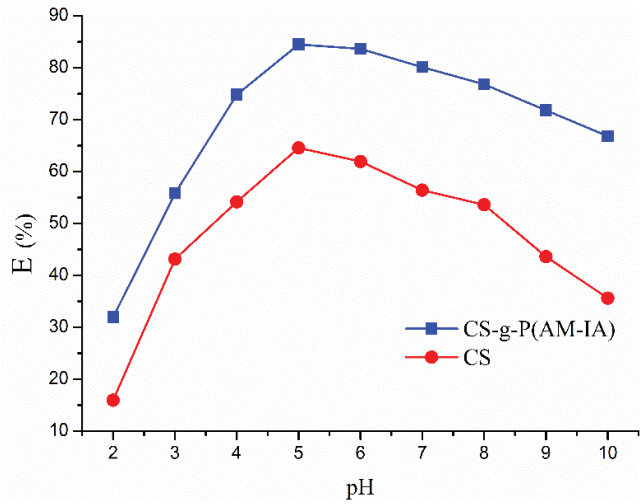

Fig. 7. Effect of pH on the Pb^{2+} removal.

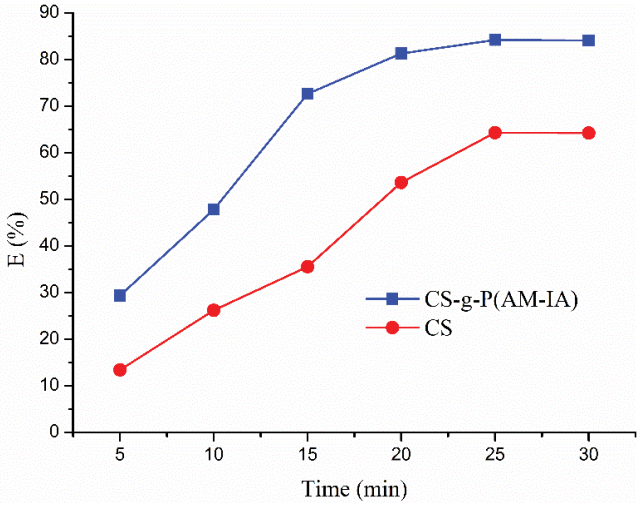

Fig. 8. Effect of flocculation time on the Pb^{2+} removal.

a large amount of Pb^{2+}. Meanwhile, these molecular chains and other molecular chains with adsorbing Pb^{2+} overlap each other to form a network structure, which increases the contact opportunities with Pb^{2+} and improves the efficiency of Pb^{2+} adsorption and flocculation [9]. This rapid adsorption and flocculation efficiency of CS-g-P(AM-IA) indicates its good potential for application in emergency water pollution decontamination treatment. Therefore, 25 min is chosen as the optimum flocculation time for adsorption, chelation and flocculation of Pb^{2+}.

3.3.4. Influence of ionic strength and coexisting cation

In order to evaluate the interaction between Pb^{2+} and flocculant, the adsorption and flocculation effect of flocculant on Pb^{2+} ion under different ionic strength and different cation coexisting environment was investigated. The concentrations of 20, 40, 60, 80 and 100 mmol/L Na^+ ions were used respectively to simulate the different ionic strengths of the practical water samples. 50 mmol/L of Na^+, K^+, Ca^{2+} and Mg^{2+} were used to simulate the coexisting cations of the natural water body. As shown in Fig. 9, the removal rate of Pb^{2+} by flocculants declined with the increase of Na^+ ion concentration. That is to say, with the increase of ion strength, the adsorption and coagulation capacity of the flocculant decreases. It is mainly due to the adhesion, adsorption and chelation of Pb^{2+} ions by flocculants s, and the existence of ion-exchanges and electrostatic interactions in flocculation [52]. It is worth noting that there are also ionic active groups on CS, whose adsorption and coagulation efficiency for Pb^{2+} are also affected by ionic strength. In addition, different coexisting cations have different degrees of influence on the flocculation and adsorption of Pb^{2+}, and the order of influence is followed by $Ca^{2+} > Mg^{2+} > K^+ > Na^+$. It is obvious that divalent cations have stronger affinity for ionic active groups in flocculants than monovalent cations, and can form stable complexes with –COO– and $–NH_2$. Consequently, it competes with the Pb^{2+} for the active groups on the flocculants and caused a reduction in Pb^{2+} chelation and adsorption [53].

3.3.5. Heavy metal flocs size and fractal dimension

When the flocculant dosage is low, the flocculant molecular chains do not completely contact with heavy metal colloids or suspended particles. With the increase of flocculant dosage, the chelating flocculation of heavy metal ions was enhanced, which accelerated the chelates capture and enhanced the flocculation performance, as well as improved the removal efficiency of Pb^{2+}. After the addition of excessive flocculant, Pb^{2+} colloidal and particles formed by chelating– flocculation will have excessive negative charges on their surface, which will lead to the enhancement of electrostatic repulsion among particles or between particles and flocculant. It reduces the probability of particle collision, and results in the decrease of flocculation efficiency. As can be found from Fig. 10a and b, under the optimal dosage (3.0 mg/L), the particle size and fractal dimension of the Pb^{2+} flocs by CS-g-P(AM-IA) are the largest. The Pb^{2+} flocs size (d_{50}) is 275.9 μm, and its D_f reaches 1.91. The reason is that CS-g-P(AM-IA) contains active $–NH_2$, hydroxyl and carboxyl groups with strong adsorption. When the active adsorption groups of CS-g-P(AM-IA) contacts with Pb^{2+}, coordination and chelation will rapidly occur, and Pb^{2+} ions are fixed on the CS-g-P(AM-IA) molecular chains. Subsequently, with more and more heavy metal ions captured by adsorption and chelation, CS-g-P(AM-IA) molecular chain aggregates and clusters together to result in efficient flocculation [54,55]. Finally, large and dense heavy metal flocs forms, and then precipitates and separates rapidly. CS-g-P(AM-IA) has high efficiency in removing Pb^{2+} ions, and shows a huge market application prospect.

3.3.6. Mechanisms of heavy metal chelation and flocculation

As seen in Fig. 11, the Pb^{2+} removal firstly depends on the chelating groups (mainly carboxylic acids) in CS-g-P(AM-IA) by various effects such as coordination complexation, electrostatic attraction and chelation [56]. Under those effects, Pb^{2+} is efficiently immobilized and precipitated, resulting in the original tiny heavy metal chelated floc particles.

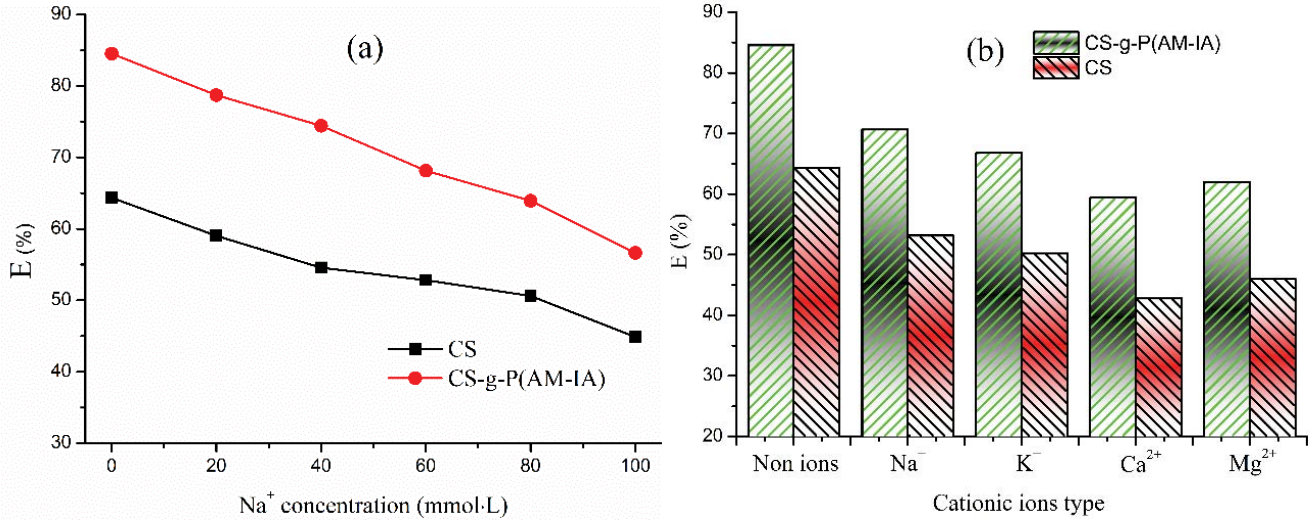

Fig. 9. Effect of ionic strength (a) and cationic type (b) on the Pb^{2+} removal.

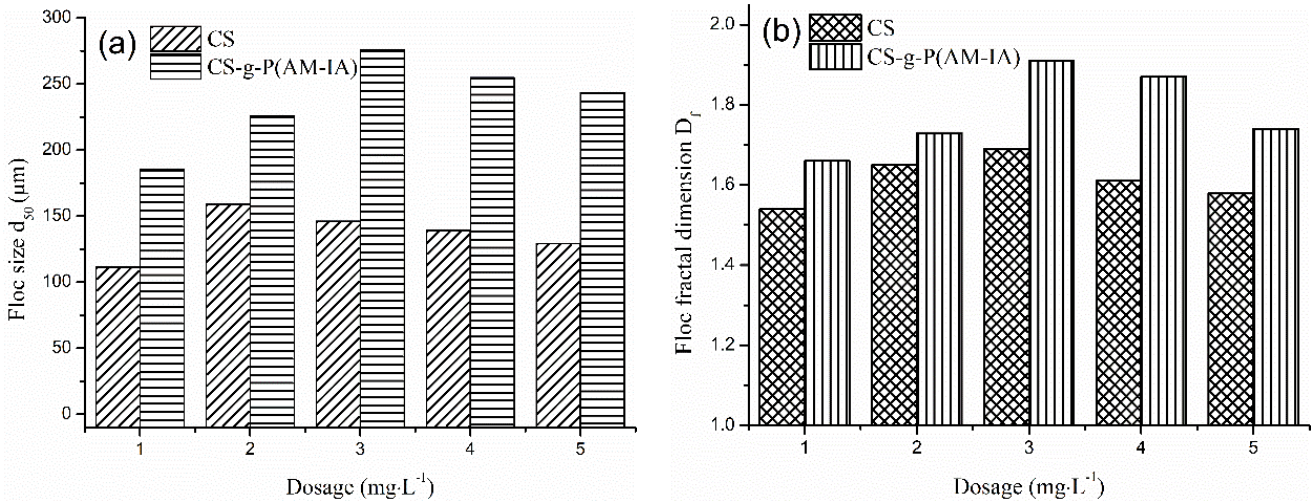

Fig. 10. Floc size d_{50} (a) and fractal dimension D_f (b).

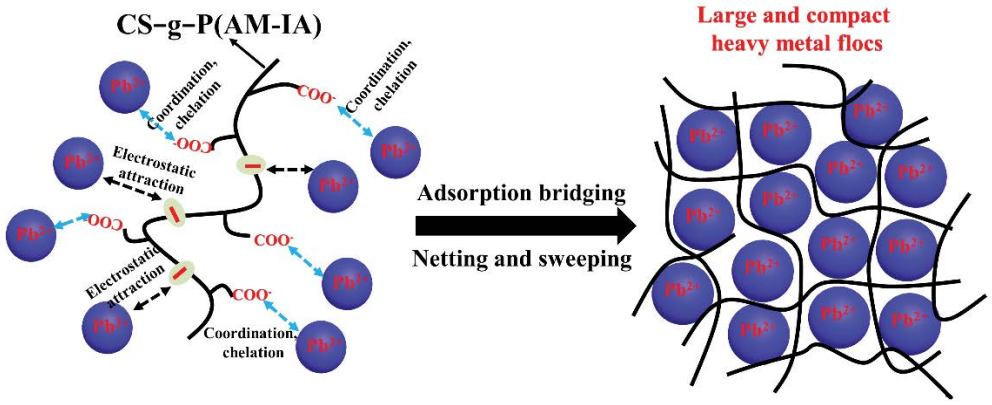

Fig. 11. Mechanism of heavy metal chelation and flocculation.

The generated tiny heavy metal flocs then aggregated and agglomerated under the adsorption bridge of the CS-g-P(AM-IA) polymer chain, then rapid flocculation occurred. The long molecular chain of CS-g-P(AM-IA) is adsorbed and wounded on the surface of the generated heavy metal flocs, and the flocculant rings and tails suspends and extends in the solution. Due to strong agitation and mixing in the flocculation process, the suspended rings and tails collided and adhered to other heavy metal particle surfaces through adsorption bridging, net catching and sweeping effects. These flocs are entangled and aggregated into large and dense particles, strengthening the separation and removal efficiency of Pb^{2+}.

4. Conclusion

In this study, AM, IA and CS were employed as monomers to prepare a new chitosan grafted polymer, namely, CS-g-P(AM-IA). CS-g-P(AM-IA) is used as a novel flocculant for heavy metal removing. The influence of single factor on the intrinsic viscosity of the grafted polymer was investigated. The effect of single factor conditions on the Pb^{2+} removal efficiency is also studied and the related Pb^{2+} removal performance is evaluated. Besides, the heavy metal flocs particle size and fractal dimension is discussed to further understand the chelation and flocculation mechanism. The main conclusions of this study are as follows.

- The intrinsic viscosity of CS-g-P(AM-IA) reached the maximum value (η = 5.54 dL/g) at the optimal react conditions (V50 concentration = 6 mol/L, the total monomer concentration = 30 wt.%, $m_{(AM+IA)}/m_{CS}$ = 4, and the ultrasonic time = 9 min).
- The results of FT-IR and TG/DSC showed that AM and IA were grafted on CS successfully. CS-g-P(AM-IA) has three stages of weight loss, and its molecular structure thermal decomposition is at 191.6°C, which has good thermal stability and is convenient for storage and application at room temperature.
- SEM results indicated that CS-g-P(AM-IA) has a larger D_f (1.329) than that of CS (1.264). CS-g-P(AM-IA) has a rough, irregular surface morphology and a large specific surface area, which is beneficial to the improvement of its solubility and adsorption properties.
- Flocculant dosage, pH and flocculation time all affect the removal performance of Pb^{2+}. At pH of 5.0, dosage

of 3.0 mg/L and stirring time of 25 min, the adsorption and flocculation effect of CS (E = 64.3%) and CS-g-P(AM-IA) (E = 84.5%) reached the optimal value. Both strong acid and strong alkalinity conditions are not conducive to the Pb^{2+} removal.

- The Pb^{2+} removal efficiency reduced with the increase of Na^+ ion concentration, and there were ion-exchange and electrostatic interactions in the coordination adsorption and chelation flocculation of Pb^{2+} ions. The coexisting cations showed adverse effects on the removal of Pb^{2+}, which was in the order of $Ca^{2+} > Mg^{2+} > K^+ > Na^+$.
- The introduction of IA and AM greatly enhanced CS-g-PAAI coordination adsorption and flocculation ability. CS-g-PAAI has strong coordination, adsorption, chelating and flocculation ability for Pb^{2+}. The generated large and compact heavy metal flocs with d_{50} of 275.9 μm and D_f of 1.91 by CS-g-PAAI greatly facilitated the efficient separation and removal of Pb^{2+}.

Acknowledgments

The authors are grateful for the financial support provided by the financial support provided by the scientific research project of Yibin Vocational Technical College (Grant No.ZRKY21ZD-07) and Key Research Base of Philosophy and Social Sciences in Sichuan Province-Sichuan Education Development Research Center of West China Normal University (Grant No.CJF16048).

References

[1] S. Basak, N. Nandi, S. Paul, I.W. Hamley, A. Banerjee, A tripeptide-based self-shrinking hydrogel for waste-water treatment: removal of toxic organic dyes and lead (Pb^{2+}) ions, Chem. Commun., 53 (2017) 5910–5913.

[2] A.R. Hernández-Martínez, G.A. Molina, L.F. Jiménez-Hernández, A.H. Oskam, G. Fonseca, M. Estevez, Evaluation of inulin replacing chitosan in a polyurethane/polysaccharide material for Pb^{2+} removal, Molecules, 22 (2017) 2093, doi: 10.3390/molecules22122093.

[3] F. Fu, Q. Wang, Removal of heavy metal ions from wastewaters: a review, J. Environ. Manage., 92 (2011) 407–418.

[4] A.M. Mohammad, T.A. Salah Eldin, M.A. Hassan, B.E. El-Anadouli, Efficient treatment of lead-containing wastewater by hydroxyapatite/chitosan nanostructures, Arabian J. Chem., 10 (2017) 683–690.

[5] S. Lu, L. Pei, A study of zinc borne waste water treatment with dispersion supported liquid membrane, Int. J. Hydrogen Energy, 35 (2016) 15717–15723.

[6] W. Liu, T. Wang, A.G.L. Borthwick, Y. Wang, X. Yin, X. Li, J. Ni, Adsorption of Pb^{2+}, Cd^{2+}, Cu^{2+} and Cr^{3+} onto titanate nanotubes: competition and effect of inorganic ions, Sci. Total Environ., 456 (2013) 171–180.

[7] V.J. Inglezakis, M.D. Loizidou, H.P. Grigoropoulou, Equilibrium and kinetic ion-exchange studies of Pb^{2+}, Cr^{3+}, Fe^{3+} and Cu^{2+} on natural clinoptilolite, Water Res., 36 (2002) 2784–2792.

[8] M. Minceva, R. Fajgar, L. Markovska, V. Meshko, Comparative study of Zn^{2+}, Cd^{2+}, and Pb^{2+} removal from water solution using natural clinoptilolitic zeolite and commercial granulated activated carbon. Equilibrium of adsorption, Sep. Sci. Technol., 43 (2008) 2117–2143.

[9] H. Wei, B. Gao, J. Ren, A. Li, H. Yang, Coagulation/flocculation in dewatering of sludge: a review, Water Res., 143 (2018) 608–631.

[10] F. Ge, M.M. Li, H. Ye, B.X. Zhao, Effective removal of heavy metal ions Cd^{2+}, Zn^{2+}, Pb^{2+}, Cu^{2+} from aqueous solution by polymer-modified magnetic nanoparticles, J. Hazard. Mater., 211 (2012) 366–372.

[11] K. Li, Y. Wang, M. Huang, H. Yan, H. Yang, S. Xiao, A. Li, Preparation of chitosan-graft-polyacrylamide magnetic composite microspheres for enhanced selective removal of mercury ions from water, J. Colloid Interface Sci., 455 (2015) 261–270.

[12] K. Zhang, Z. Wang, Y. Li, Z. Jiang, Q. Hu, M. Liu, Q. Zhao, Dual stimuli-responsive N-phthaloylchitosan-graft-(poly(N-isopropylacrylamide)-block-poly(acrylic acid)) copolymer prepared via RAFT polymerization, Carbohydr. Polym., 92 (2013) 662–667.

[13] H. Rezania, V. Vatanpour, S. Faghani, Poly(itaconic acid)-assisted ultrafiltration of heavy metal ions' removal from wastewater, Iran. Polym. J., 28 (2019) 1069–1077.

[14] D. Soto, J. Urdaneta, K. Pernia, O. León, A. Muñoz-Bonilla, M. Fernández-García, Itaconic acid grafted starch hydrogels as metal remover: capacity, selectivity and adsorption kinetics, J. Polym. Environ., 24 (2016) 343–355.

[15] T. Lü, Y. Chen, D. Qi, Z. Cao, D. Zhang, H. Zhao, Treatment of emulsified oil wastewaters by using chitosan grafted magnetic nanoparticles, J. Alloys Compd., 696 (2017) 1205–1212.

[16] X. Liang, J. Zhang, L. Du, M. Zhang, Effect of resonant tunneling modulation on ZnO/In_2O_3 heterojunction nanocomposite in efficient detection of NO_2 gas at room temperature, Sens. Actuators, B, 329 (2021) 129230, doi: 10.1016/j.snb.2020.129230.

[17] J. Qian, Y. Li, J. Gao, Z. He, S. Yi, The effect of ultrasonic intensity on physicochemical properties of Chinese fir, Ultrason. Sonochem., 64 (2020) 104985, doi: 10.1016/j.ultsonch.2020.104985.

[18] Y. Peng, C. Xia, M. Cui, Z. Yao, X. Yi, Effect of reaction condition on microstructure and properties of (NiCuZn) Fe_2O_4 nanoparticles synthesized via co-precipitation with ultrasonic irradiation, Ultrason. Sonochem., 71 (2021) 105369, doi: 10.1016/j.ultsonch.2020.105369.

[19] S. Merouani, O. Hamdaoui, Y. Rezgui, M. Guemini, Sensitivity of free radicals production in acoustically driven bubble to the ultrasonic frequency and nature of dissolved gases, Ultrason. Sonochem., 71 (2015) 105369, doi: 10.1016/j.ultsonch.2014.07.011.

[20] Y. Yu, J. Wang, Preparation of graphene/PMMA composites with assistance of ultrasonic wave under supercritical CO_2 conditions, Ultrason. Sonochem., 73 (2021) 105487, doi: 10.1016/j.ultsonch.2021.105487.

[21] A. Rayaprolu, S.K. Srivastava, K. Anand, L. Bhati, A. Asthana, C.M. Rao, Fabrication of cost-effective and efficient paper-based device for viscosity measurement, Anal. Chim. Acta, 1044 (2018) 86–92.

[22] H. Yang, Y. Yan, P. Zhu, H. Li, Q. Zhu, C. Fan, Studies on the viscosity behavior of polymer solutions at low concentrations, Eur. Polym. J., 41 (2005) 329–340.

[23] S.Y. Khor, N.P. Truong, J.F. Quinn, M.R. Whittaker, T.P. Davis, Polymerization-induced self-assembly: the effect of end group and initiator concentration on morphology of nanoparticles prepared via RAFT aqueous emulsion polymerization, ACS Macro Lett., 6 (2017) 1013–1019.

[24] Y. Hu, Y. Chen, Q. Chen, L. Zhang, X. Jiang, C. Yang, Synthesis and stimuli-responsive properties of chitosan/poly(acrylic acid) hollow nanospheres, Polymer (Guildf)., 46 (2005) 12703–12710.

[25] S. Jia, S. Jia, S. Jia, H. Pan, H. Pan, H. Pan, Q. Lin, Q. Lin, X. Wang, X. Wang, C. Li, C. Li, M. Wang, Y. Shi, Y. Shi, Study on the preparation and mechanism of chitosan-based nano-mesoporous carbons by hydrothermal method, Nanotechnology, 31 (2020) 365604, doi: 10.1088/1361-6528/ab9575.

[26] Z. Yang, H. Li, H. Yan, H. Wu, H. Yang, Q. Wu, H. Li, A. Li, R. Cheng, Evaluation of a novel chitosan-based flocculant with high flocculation performance, low toxicity and good floc properties, J. Hazard. Mater., 276 (2014) 480–488.

[27] J. Pan, J. Zhu, F. Cheng, Preparation of sodium lignosulfonate/chitosan adsorbent and application of Pb^{2+} treatment in water, Sustainability, 13 (2021) 2997.

[28] B.L. Liao, J. Xu, M.N. Ren, F.H. Cao, Modified chitosan with wide flocculation window for removing emulsified oil in petroleum wastewater, Xiandai Huagong/Modern Chem. Ind., 41 (2021) 203–208.
[29] M.R. Gopal Reddi, T. Gomathi, P.N. Sudha, Synthesis and characterization of graft copolymerization of chitosan with ethylene dimethacrylate, Der Pharm. Lett., 38 (2014) 2455–2462.
[30] A. Pourjavadi, G.R. Mahdavinia, M.J. Zohuriaan-Mehr, H. Omidian, Modified chitosan. I. Optimized cerium ammonium nitrate-induced synthesis of chitosan-graft-polyacrylonitrile, J. Appl. Polym. Sci., 88 (2003) 2048–2054.
[31] P. Wu, J. Yi, L. Feng, X. Li, Y. Chen, Z. Liu, S. Tian, S. Li, S. Khan, Y. Sun, Microwave assisted preparation and characterization of a chitosan based flocculant for the application and evaluation of sludge flocculation and dewatering, Int. J. Biol. Macromol., 155 (2020) 708–720.
[32] L. Chen, Y. Sun, W. Sun, K.J. Shah, Y. Xu, H. Zheng, Efficient cationic flocculant MHCS-g-P(AM-DAC) synthesized by UV-induced polymerization for algae removal, Sep. Purif. Technol., 210 (2019) 10–19.
[33] T. Lou, G. Cui, J. Xun, X. Wang, N. Feng, J. Zhang, Synthesis of a terpolymer based on chitosan and lignin as an effective flocculant for dye removal, Colloids Surf., A, 537 (2018) 149–154.
[34] Y. Sun, C. Zhu, W. Sun, Y. Xu, X. Xiao, H. Zheng, H. Wu, C. Liu, Plasma-initiated polymerization of chitosan-based CS-g-P(AM-DMDAAC) flocculant for the enhanced flocculation of low-algal-turbidity water, Carbohydr. Polym., 164 (2017) 222–232.
[35] R. Jalilian, M. Shahmari, A. Taheri, K. Gholami, Ultrasonic-assisted micro solid phase extraction of arsenic on a new ion-imprinted polymer synthesized from chitosan-stabilized pickering emulsion in water, rice and vegetable samples, Ultrason. Sonochem., 61 (2020) 104802.
[36] S. Ansari, S. Masoum, Ultrasound-assisted dispersive solid-phase microextraction of capecitabine by multi-stimuli responsive molecularly imprinted polymer modified with chitosan nanoparticles followed by HPLC analysis, Microchim. Acta, 187 (2020) 366, doi: 10.1007/s00604-020-04345-0.
[37] S.R. Patel, M.P. Patel, Green and facile preparation of ultrasonic wave-assisted chitosan-g-poly-(AA/DAMPB)/Fe_3O_4 composite hydrogel for sequestration of reactive black 5 dye, Polym. Bull., 79 (2022) 3193–3217.
[38] L. Feng, X. Li, W. Lu, Z. Liu, C. Xu, Y. Chen, H. Zheng, Preparation of a graft modified flocculant based on chitosan by ultrasonic initiation and its synergistic effect with kaolin for the improvement of acid blue 83 (AB 83) removal, Int. J. Biol. Macromol., 150 (2020) 617–630.
[39] P. Zhang, D.Q. Zhao, Characterization and dimethyl phthalate flocculation performance of the cationic polyacrylamide flocculant P(AM-DMDAAC) produced by microwave-assisted synthesis, Molecules, 25 (2020) 624, doi: 10.3390/molecules25030624.
[40] Y. Ni, J. Yi, Research on improving the surface hydrophobicity of paper coated by poly-vinyl alcohol-itaconic acid grafting copolymer, Prog. Org. Coat., 31 (2019) 152–158.
[41] Z. Zhang, H. Zheng, F. Huang, X. Li, S. He, C. Zhao, Template polymerization of a novel cationic polyacrylamide: sequence distribution, characterization, and flocculation performance, Ind. Eng. Chem. Res., 55 (2016) 9819–9828.
[42] X. Li, H. Zheng, B. Gao, Y. Sun, B. Liu, C. Zhao, UV-initiated template copolymerization of AM and MAPTAC: Microblock structure, copolymerization mechanism, and flocculation performance, Chemosphere, 167 (2017) 71–81.
[43] L. Feng, H. Zheng, X. Tang, X. Zheng, S. Liu, Q. Sun, M. Wang, The investigation of the specific behavior of a cationic block structure and its excellent flocculation performance in high-turbidity water treatment, RSC Adv., 8 (2018) 15119–15133.
[44] Y. Sun, M. Ren, C. Zhu, Y. Xu, H. Zheng, X. Xiao, H. Wu, T. Xia, Z. You, UV-initiated graft copolymerization of cationic chitosan-based flocculants for treatment of zinc phosphate-contaminated wastewater, Ind. Eng. Chem. Res., 55 (2016) 10025–10035.
[45] L. Feng, S. Liu, H. Zheng, J. Liang, Y. Sun, S. Zhang, X. Chen, Using ultrasonic (US)-initiated template copolymerization for preparation of an enhanced cationic polyacrylamide (CPAM) and its application in sludge dewatering, Ultrason. Sonochem., 44 (2018) 53–63.
[46] J. Cao, S. Zhang, B. Han, Q. Feng, L.F. Guo, Characterization of cationic polyacrylamide-grafted starch flocculant synthesized by one-step reaction, J. Appl. Polym. Sci., 123 (2012) 1261–1266.
[47] Y. Bagbi, A. Sarswat, D. Mohan, A. Pandey, P.R. Solanki, Lead (Pb^{2+}) adsorption by monodispersed magnetite nanoparticles: Surface analysis and effects of solution chemistry, J. Environ. Chem. Eng., 4 (2016) 4237–4247.
[48] Z. Wang, J. Nan, M. Yao, Y. Yang, Effect of additional polyaluminum chloride and polyacrylamide on the evolution of floc characteristics during floc breakage and re-growth process, Sep. Purif. Technol., 173 (2017) 144–150.
[49] T. Wang, W. Liu, L. Xiong, N. Xu, J. Ni, Influence of pH, ionic strength and humic acid on competitive adsorption of Pb(II), Cd(II) and Cr(III) onto titanate nanotubes, Chem. Eng. J., 215 (2013) 366–374.
[50] G. Sheng, S. Wang, J. Hu, Y. Lu, J. Li, Y. Dong, X. Wang, Adsorption of Pb(II) on diatomite as affected via aqueous solution chemistry and temperature, Colloids Surf., A, 339 (2009) 159–166.
[51] S.W. Yu, H.J. Choi, Application of hybrid bead, persimmon leaf and chitosan for the treatment of aqueous solution contaminated with toxic heavy metal ions, Water Sci. Technol., 78 (2018) 837–847.
[52] C. Xu, Y. Shan, M. Bilal, B. Xu, L. Cao, Q. Huang, Copper ions chelated mesoporous silica nanoparticles via dopamine chemistry for controlled pesticide release regulated by coordination bonding, Chem. Eng. J., 395 (2020) 125093, doi: 10.1016/ j.cej.2020.125093.
[53] S. Chen, W. Shen, F. Yu, H. Wang, Kinetic and thermodynamic studies of adsorption of Cu^{2+} and Pb^{2+} onto amidoximated bacterial cellulose, Polym. Bull., 63 (2009) 283–297.
[54] Z. Li, Y. Gong, D. Zhao, Z. Dang, Z. Lin, Enhanced removal of zinc and cadmium from water using carboxymethyl cellulose-bridged chlorapatite nanoparticles, Chemosphere, 263 (2021) 128038, doi: 10.1016/j.chemosphere.2020.128038.
[55] Z. Yin, L. Zhu, F. Mo, S. Li, D. Hu, R. Chu, C. Liu, C. Hu, Preparation of biochar grafted with amino-riched dendrimer by carbonization, magnetization and functional modification for enhanced copper removal, J. Taiwan Inst. Chem. Eng., 121 (2021) 349–359.
[56] Y. Huang, D. Wu, X. Wang, W. Huang, D. Lawless, X. Feng, Removal of heavy metals from water using polyvinylamine by polymer-enhanced ultrafiltration and flocculation, Sep. Purif. Technol., 158 (2016) 124–136.